Limnol. Oceanogr., 50(1), 2005, 184–196

Cold intrusions in Lake Baikal: Direct observational evidence for deep-water renewal

Alfred Wüest[1] *and Thomas M. Ravens*
Limnological Research Center, EAWAG; Seestrasse 79, CH-6047 Kastanienbaum, Switzerland

Nikolai G. Granin
Limnological Institute of the Siberian Division of the Russian Academy of Sciences, P.O. Box 4199, Irkutsk 664033, Russia

Otti Kocsis, Michael Schurter, and Michael Sturm
Limnological Research Center, EAWAG; Seestrasse 79, CH-6047 Kastanienbaum, Switzerland

Abstract

We studied cold, deep-water intrusions in the South Basin of Lake Baikal on the basis of 2 yr of data (December 1995–November 1997) from near-bottom and near-surface thermistor strings, monthly conductivity–temperature–depth (CTD) profiles, and a near-bottom current meter, all collected near the South Basin maximum depth of 1,461 m. The data show intrusions into the greatest depths with temperatures of 0.08–0.20°C below ambient (~3.33 to ~3.38°C at maximum depth). The intrusions were observed three times per year between January and June, when surface water is always cooler than deep water, with durations of a few (at least 1–3) days. The estimated water input ranged from 1 to 10 km^3 per event, and the annually accumulated volume was estimated to be 10–30 km^3, which is significantly less than the steady-state indirect estimates of 30–70 $km^3\ yr^{-1}$ to the permanently stratified deep water (depth > 300 m). This indicates that not all of the cold intrusions reach the deepest area. Because the cooling of the near-bottom waters was not accompanied by a significant increase in ion or particle content and because deep sediment traps did not contain significant enrichments of minerogenic particles, we concluded that Selenga River inflow is not a possible source of the cold intrusions. Two CTD profiles in June 1996 and 1997 showed lower temperature throughout the deep water, as expected from thermobaric instabilities. The required downwelling is definitely not occurring in the pelagic interior but most probably by near-coast counterclockwise currents. The source of the regularly occurring deep intrusions is clearly cold surface water, but the actual mechanism is uncertain.

Vertical mixing in Lake Baikal (Fig. 1), the deepest lake on earth (1,642 m; Intas Project Team 2002), is surprisingly efficient. Despite its great depth, oxygen concentrations are high (>9.5 mg L^{-1}) throughout the water column (Shimaraev et al. 1994; Beeton 2002), and the tritium/helium and chlorofluorocarbon (CFC) water ages, respectively, are less than 20 yr old (Weiss et al. 1991; Hohmann et al. 1998; Kodenev 2001). The ''young'' age of the water at such great depth was not at all expected. The short residence timescale of the deep water is particularly surprising, given that the water column in Lake Baikal shows a permanent stratification below ~300 m depth. Obviously, this permanently stratified deep water (PSDW) is not stagnant, as in many meromictic lakes, but experiences significant vertical exchange.

The exchange of PSDW with the overlaying surface water is a result of two different types of processes: efficient diffusive mixing (Ravens et al. 2000) of turbulent eddies over scales of up to tens of meters (Lorke and Wüest 2002) and episodic, advective-type, large-scale, deep-water intrusion events (Hohmann et al. 1997; Kodenev et al. 1998). These two types of transport, which are both ''renewing'' the deep water, control the vertical heat, mass, and density fluxes and thereby maintain their respective vertical gradients, and subsequently the long-term stratification, in the PSDW.

In the South Basin, the PSDW is stratified mainly because of a mild temperature gradient, ranging from ~3.50°C at 300 m depth to ~3.35°C in the deepest reaches. Ions and silica contribute little to the stratification (Shimaraev and Domysheva 2002). Because small-scale turbulence is a ubiquitous process in all natural waters (Wüest and Lorke 2003), this PSDW temperature gradient (Fig. 2) causes heat to diffuse downward (countergradient), continuously warming the deepest water. This heat flux would increase the temperature in the PSDW (and thereby eliminate the stratification) in the long run if there were not a process to cool the deep water. That such a warming has not been observed over many de-

[1] Corresponding author (e-mail: Wuest@eawag.ch).

Acknowledgments

We are indebted to Ruslan Gnadovsky and Rolf Kipfer for organizational support. Also, we thank the members of the Limnological Institute, Irkutsk, for providing logistical support—especially the crews of the RV *Vereschagin* and RV *Titov*. Eliane Scharmin and Lorenz Moosmann contributed to the preparation of the manuscript and the figures. Martin Schmid and Martin Vollmer reviewed an earlier version of the manuscript. We also acknowledge the constructive input given by two anonymous reviewers. The Swiss Federal Office for Education and Science, the British National Environmental Research Council, and the Swiss Federal Institute for Environmental Sciences and Technology (EAWAG) contributed to the mooring field work. The CTD work was supported by the Royal Society of London and the Siberian Branch of the Russian Academy of Sciences. T.M.R. and N.G.G. received grants from the Swiss National Science Foundation projects 20-36′364.92, 2000-43′357.95, and 20-50′761.97.

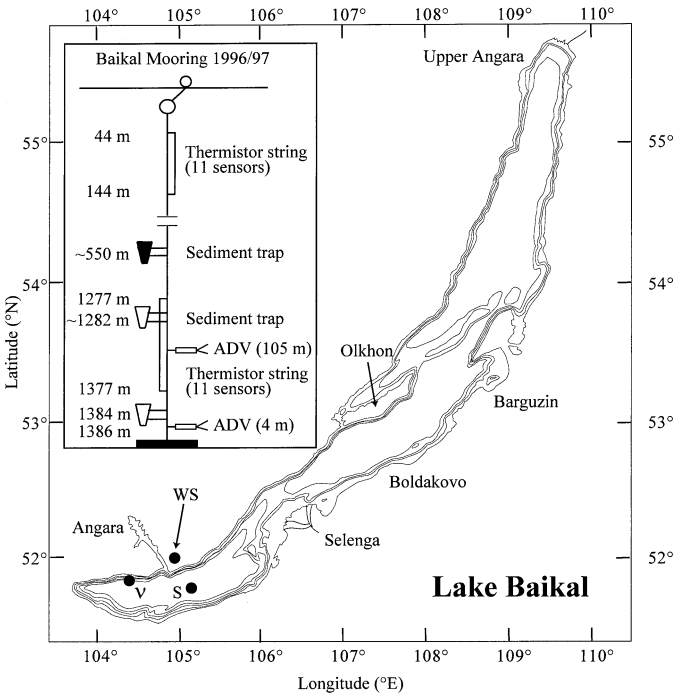

Fig. 1. Lake Baikal map: ''S'' (51°41′48″N, 105°3′10″E) indicates the location of the mooring that is the subject of this paper. ν marks the later mooring (Neutrino experiment; not discussed here). WS indicates the permanent weather station at the South Basin. The inset displays the depth levels of the two thermistor strings, the acoustic Doppler velocity (ADV) current meter, and the sediment traps at station S during the 1996 and 1997 deployments.

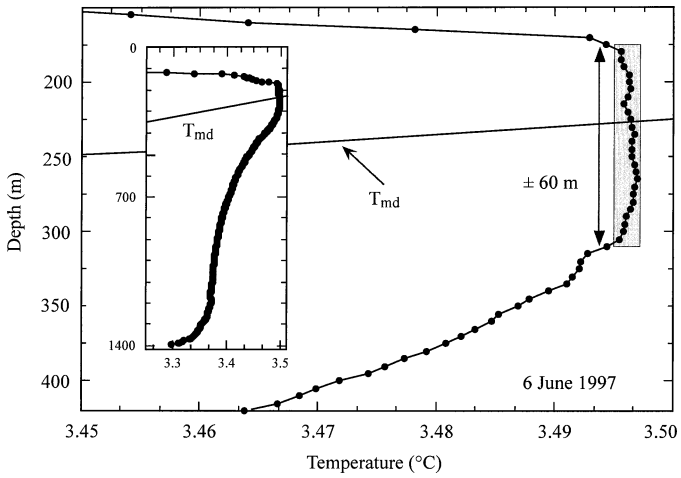

Fig. 2. Temperature profile from 6 June 1997 indicating the cold and inversely stratified surface layer (above 200 m depth), the permanently stratified deep water (PSDW, below 300 m depth) and the homogenized layer of the mesothermal temperature maximum around the line of temperature of maximum density, T_{md}. The uniformity is a result of mixing by thermobaric instability. Inset shows the entire temperature profile and indicates the near-bottom temperature of $T \approx 3.35$°C.

cades (Shimaraev et al. 1994) implies that cooling occurs at least every few years. In this paper, we present the first direct evidence of such cold, deep-water intrusions into the South Basin of Lake Baikal. Although we cannot determine the exact origin of these cold intrusions, it is certain that they contain colder water from above the PSDW.

On the basis of observational evidence, we assume that the temperature in the PSDW is near steady state and that vertical diffusion and the deep-water intrusions balance the heat content of the PSDW.

On the basis of such a heat budget, vertical diffusivity constrains the heat loss to be expected by the cold intrusions. In Lake Baikal, vertical diffusivity (K_z) has been studied with temperature microstructure and inertial dissipation measurements (Ravens et al. 2000), with the use of temperature profiles (Shimaraev and Granin 1991; Ravens et al. 2000), and CFCs, ^{3}H, ^{3}He, or dissolved oxygen as tracers (Killworth et al. 1996; Peeters et al. 2000), as well as with temperature profile modeling (Lawrence et al. 2002) and by balancing biogeochemical water constituents (Wüest et al. 2000). The various methods employed lead to K_z estimates of 1–90 cm^2 s^{-1}, indicating an extremely efficient vertical diffusivity for the PSDW. (The only exception is Killworth et al. [1996], who determined a K_z of 0.05 cm^2 s^{-1}, which has been shown in the meantime to be unreasonably small [Peeters et al. 2000; Ravens et al. 2000; Lawrence et al. 2002].) The vertical diffusivity of tens of cm^2 s^{-1} in the PSDW of Lake Baikal is orders of magnitude larger than the classical open ocean value of 0.1 cm^2 s^{-1} (Ledwell et al. 1998) and 0.001–1 cm^2 s^{-1} typically found in lakes (Wüest and Lorke 2003). The reason for the exceptionally large diffusivity is the very weak stability of the water column, which allows for the existence of much larger turbulent eddies than usually found in stratified natural waters (Lorke and Wüest 2002).

The cited tracer work is particularly valuable because the inverse models employed yield not only K_z estimates but also rates of deep-water renewal (e.g., 30–100 km^3 yr^{-1}; Peeters et al. 2000; Wüest et al. 2000). However, the existing estimates of vertical deep-water replacement, inferred from tracer balancing and heat budgeting for steady-state conditions were based on indirect evidence. Furthermore, the processes leading to the penetration of the permanently stratified water column in Lake Baikal remained unidentified.

For Lake Baikal, different deep-water renewal processes have been proposed, including thermobaric instability (Carmack and Weiss 1991; Weiss et al. 1991; Crawford and Collier 1997), wind-induced currents (Botte and Kay 2002), density currents induced by the Selenga River (Hohmann et al. 1997), thermal bars (Shimaraev et al. 1993), and water exchange over the sill between the Central and North Basins at Academician Ridge (Peeters et al. 1996; Hohmann et al. 1997). In the South Basin, in particular, the most likely deep-water renewal processes are thermobaric instabilities and Selenga River–induced density currents. For example, Walker and Watts (1995) used a numerical model to demonstrate that thermobaric instability could lead to deep-water renewal given a locally sufficient vertical displacement of some thermocline water masses. According to their model results, a flow ''chimney'' could be established that would lead to transport from the near-surface layer, through the PSDW, to the deepest reaches of the lake. Also, Hohmann et al. (1997) provided evidence suggesting that Selenga River–induced

Table 1. Vertical level of moored instruments at position S (local depth = 1,390 m; GPS position = 51°41′48″ N, 105°03′10″E).

Deployment period	Current meter (height above bottom), h (m)	Bottom thermistor string (height above bottom), h_1–h_{11} (m)	Surface thermistor string (depth) z_1–z_{11} (m)	Sediment trap depths, S_1 and S_2 (m)*	No. of CTD profiles†
8 Dec 1995 to 26 Jun 1996	105‡	4–104	None	560, 1,281	8
28 Jun 1996 to 11 Dec 1996	4	13—113	44—144	522, 1,384	6
12 Dec 1996 to 8 Jul 1997	4	13—113	44—144	555, 1,384	8
9 Jul 1997 to 26 Nov 1997	105	105§	44—144	554, 1,283	4

* The deep trap was approximately 109 m above bottom in the first and fourth deployment and 6 m above bottom in the second and third deployment.
† The 26 dates of the CTD profiles were: 10 Dec 95, 10 Jan 96, 5 Mar 96, 28 Mar 96, 18 May 96, 28 May 96, 3 Jun 96, 26 Jun 96, 19 Jul 96, 20 Aug 96, 22 Aug 96, 13 Sep 96, 23 Oct 96, 11 Dec 96, 12 Dec 96, 13 Mar 97, 22 Mar 97, 1 Apr 97, 22 May 97, 6 Jun 97, 20 Jun 97, 8 Jul 97, 9 Jul 97, 15 Aug 97, 9 Sep 97, 26 Nov 97.
‡ Current meter failed on 4 May 96 (data available from 8 Dec 1995 to 3 May 1996).
§ Bottom thermistor string failed during last deployment; one record at 105 m height only.

density currents might renew the deep water of the South Basin. Other deep-water renewal mechanisms are less likely. For example, water exchange at the sill between the South and Central Basins is, in principle, possible, although temperature and salinity profiles indicate relatively little potential for such exchange (Peeters et al. 1996).

Despite the clear observational evidence from the steady PSDW heat balance, there has been little direct evidence for deep renewal. Hohmann et al. (1997) presented some conductivity–temperature–depth (CTD) profiles, which indicated intruding density flows at medium depth in the Central Basin, and Shimaraev et al. (1993) showed some cold-water penetration events at medium depth in the Central Basin.

In this paper, we present near-bottom thermistor chain, velocity, and CTD data from the South Basin, which provide the first direct evidence of cold, deep-water intrusions into Lake Baikal. These data enable a rough estimate of the replacement volume required to maintain the long-term temperature and stratification of the PSDW of the South Basin. In addition, the potential role of the thermobaric instability is discussed. We close the paper with an evaluation of possible mechanisms potentially responsible for such ''cold intrusions,'' as we call these deep-water inputs throughout the rest of the paper.

Experimental set-up

The aim of the presented in situ observations was to gather direct evidence for cold intrusions in the South Basin, to study their temporal structure, and to make rough estimates of the volumes involved. Four different types of measurements were made. First, thermistor chains (Aanderaa Instruments) were deployed in 1996 and 1997 in the near–surface water (44–144 m depth) and in the near bottom (between 13 [or 4] and 113 [or 104] m above the local lake floor; Table 1; Fig. 1). The location of the mooring is indicated by ''S'' in Fig. 1. This site, in 1,390-m-deep water, is near the deepest location in the South Basin, with a maximum depth of 1,461 m. Second, near-bottom currents were measured by an acoustic Doppler velocity meter (SACM3, EG&G Marine Instruments), as described in Ravens et al. (2000). Third, CTD profiles (SBE-25, SeaBird), including optical backscattering (OBS-1, D&A), were collected on 26 occasions during this 2-yr time period (Table 1). Finally, sequencing sediment traps (Technicap-PPS 4/3), with an active area of 500 cm^2, were installed at about 550 and 1,300 m depth (Fig. 1). The collecting cups in the two sequencing traps were automatically replaced approximately every 2 weeks. The detailed information on time periods, depth levels (also in Fig. 1), and collected data for the four deployments is summarized in Table 1.

In this paper, we have difficulty providing well-defined error bars for the volume estimates of the cold intrusions, but not because of errors in the collected data, which we consider negligibly small. The errors are about 0.002 °C, 0.01 °C and 0.02 °C for temperatures from the CTD, the deep thermistors, and the shallow thermistors, respectively, a few millimeters per second for the acoustically measured currents, and about 10% for the sedimentation rate estimates. The error bars that we provide are based on uncertainty about our ability to represent the measurements. This uncertainty is unavoidable because we have only one mooring. The only option we see is to use all the arguments and data to constrain the intrusion volume estimates.

The calculation of the density, ρ, is performed according to Chen and Millero (1986), with the salinity as determined from in situ CTD conductivity by the Wüest et al. (1996) procedure. The stability of the stratification $N^2 = -g\rho^{-1}(\partial\rho/\partial z)$, where ρ is the density calculated for depth $z = 0$, can be approximated by $g\alpha[(\partial T/\partial z) - \Gamma]$ in the South Basin because the salinity and silicic acid contribute little to the stratification compared with the temperature T ($g = 9.81$ m s^{-2}, $\alpha = -\rho^{-1}[\partial\rho/\partial T]$ is the thermal expansivity, Γ is the adiabatic temperature gradient, and z [m] is the water depth defined as positive upward with $z = 0$ at the surface). The difference between the in situ and potential temperature is only a few 0.001 °C. For simplicity, the figures show the in situ temperature.

Thermobaric instability—Stratification of the Lake Baikal waterbody has some peculiarities specific to cold, deep lakes. Throughout the warm season, the lake shows the ''classical'' stratification with (1) temperatures T above the depth (pressure)-dependent temperature of maximum density, T_{md} =

3.984°C + 0.0021*z* (line in Fig. 2), and (2) decreasing temperature with depth. The thermal expansivity $\alpha > 0$ and the water column is stably stratified, as is common in temperate lakes.

In the cold season, however, the temperature stratification has a fascinating structure, which leads to a special form of convective instability (Shimaraev and Granin 1991; Crawford and Collier 1997). For more than half of the year (approximately 3½ months of ice cover), the surface water cools from above and stratifies the uppermost water column (Fig. 2). Because T_{md} is ~4°C at atmospheric pressure, the cooler surface water is lighter and floats on the warmer, and therefore heavier, water below (i.e., thermal expansivity, $\alpha < 0$). The lower bound of the surface layer is determined by the temperature of maximum density T_{md}, which is a function of depth (as defined previously). The reason that the maximal vertical extent of the surface layer is related to T_{md} becomes evident from Figs. 2 and 3.

Below the PSDW, is not much affected by the seasonal changes at the surface, and it remains classically stratified throughout the year, with temperatures above T_{md}. The requirement for stable stratification implies that the vertical temperature gradient changes sign exactly at the depth at which the in situ temperature meets T_{md} (there, $\alpha = 0$), as exemplified in Fig. 2. Evidently, at this crossover, the temperature has its local maximum (by definition, because $\partial T/\partial z$ changes sign; Figs. 2, 3), the so-called mesothermal maximum (Shimaraev et al. 1994).

As explained in Fig. 3, this is the only temperature profile that is consistent with stable stratification. Any vertical displacement of the mesothermal maximum away from the T_{md} line leads locally to a so-called thermobaric instability, which is a specific form of convective turbulence. This instability is caused by the pressure dependency of the thermal expansivity, α. The mechanism is schematically explained in Fig. 3. Consider the stable temperature profile in the upper panel with the mesothermal maximum on the T_{md} line (Fig. 3a): If there is an upward displacement of the water column (i.e., a baroclinic uplift as indicated by the dotted line in Fig. 3b), the fluid between the mesothermal maximum and T_{md} has a negative thermal expansivity (i.e., $\alpha < 0$ compared with $\alpha > 0$ before the uplift) and is subsequently unstable throughout the grey-shaded layer in Fig. 3b. The stability $N^2 = g\alpha[(\partial T/\partial z) - \Gamma] \approx g\alpha(\partial T/\partial z)$ is negative by definition because the temperature gradient $\partial T/\partial z$ remains positive, whereas α changes to negative. A symmetrical situation results from a downward baroclinic displacement of the water (Fig. 3c). In the grey-shaded layer, the temperature gradient remains negative, whereas α changes to positive, and subsequently, the stability N^2 is again negative. From the schematic in Fig. 3, we can generalize that the fluid between the mesothermal maximum and the T_{md} line is always unstable.

From this result, we can draw two conclusions. First, the mesothermal maximum will be exposed to some weak convective turbulence most of the time because the water column is never at rest and some baroclinic motion occurs during all seasons. Therefore, the mesothermal maximum is not a well-defined maximum, but rather a well-mixed layer of almost homogeneous temperature (Fig. 2). Second, the thickness of the well-mixed layer provides an indication for the largest amplitudes of the vertical baroclinic displacement at that depth. Particularly in June, at the end of the inversely stratified winter period, the aftermath of thermobaric instability is well documented in the CTD profiles.

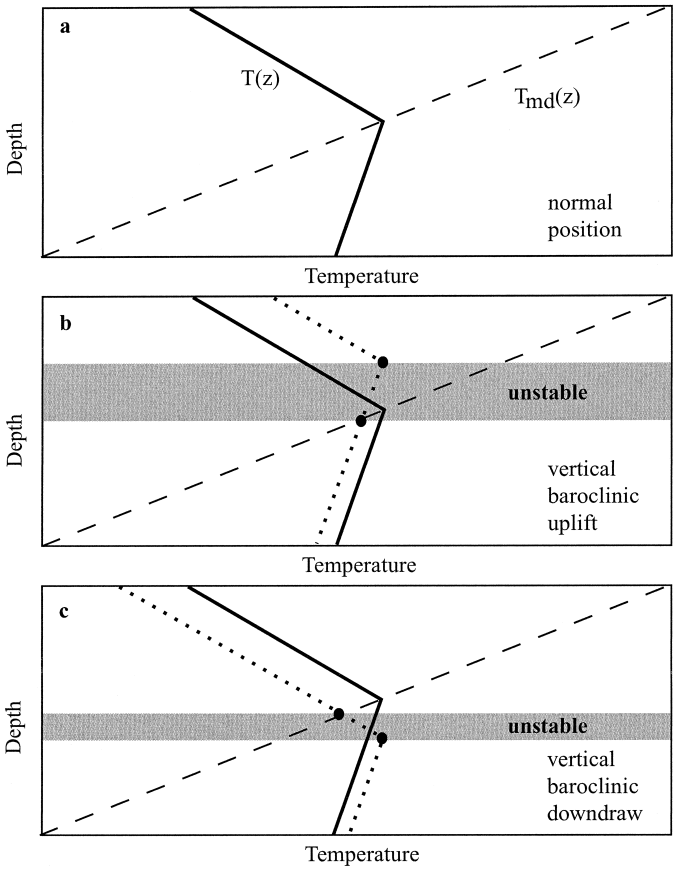

Fig. 3. Schematic of the generation of thermobaric instabilities in the top 350 m of Lake Baikal during winter and spring. (a) Idealized stable situation, T and T_{md} cross at mesothermal maximum; (b) instability caused by a baroclinic uplift; (c) instability caused by a baroclinic downdraw. Detailed explanation is in text.

From Fig. 2 we can conclude that the vertical displacements at 300 m were limited to ±60 m relative to the equilibrium depth during winter/spring 1997. If one imagines the temperature profile being displaced more than 60 m downward (upward), then the T_{md} line would lay above (below) the well-mixed layer. As a consequence, this layer would be lighter (heavier) and subsequently move up (down) to the T_{md} line and thereby expand the well-mixed layer (same argument as in Fig. 3). According to such reasoning, Fig. 2 implies that vertical displacements are limited to only ~60 m. Such maximum vertical displacements are confirmed by thermistor chain data (*see* Discussion).

From these considerations, we can conclude that thermobaric instabilities in the pelagic interior of the South Basin (site of the mooring; Fig. 1) are not a mechanism for the investigated cold intrusions. There, the induced convection never reached deeper than about 300 m. However, it is, at least in principle, possible that water bodies of limited horizontal extent could be displaced vertically much farther,

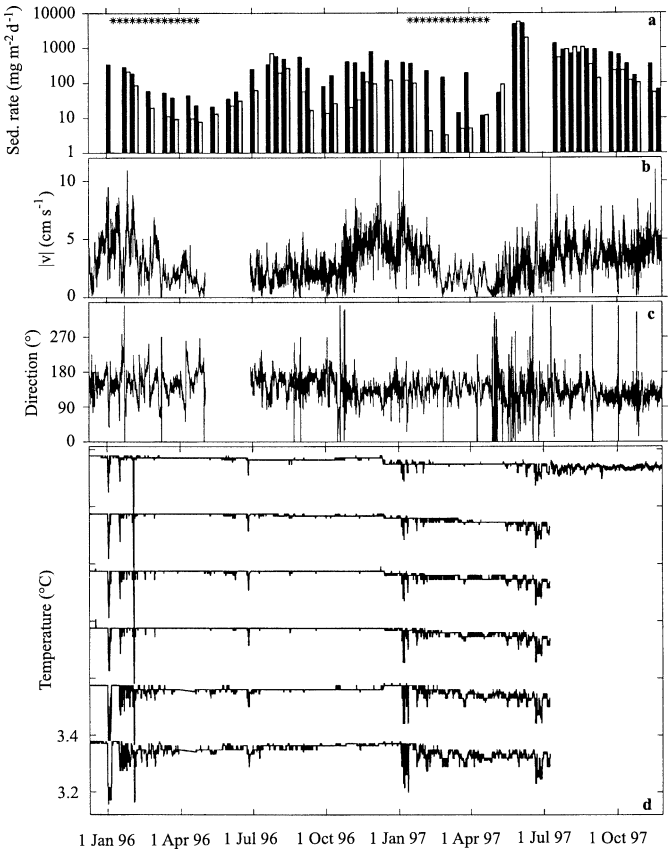

Fig. 4. (a) Averages (17-d) of vertical particle flux collected with sedimentation traps at S in ~550 m depth (open bars) and ~1,300 m depth (filled bars). Exposure periods and trap depths are given in Table 1. The horizontal lines of asterisks mark the periods of ice cover. (b) Speed of the near-bottom currents during the four deployments of the ADV current meter. From 4 May to 28 June 1996, the sensor was inoperable. Exposure periods and ADV depths are given in Table 1. (c) Direction of bottom currents at S (0° = 360° = north, 90° = east). (d) Temperature at S within the bottom 120 m as an offset-plot with 0.20°C increments. The six lines correspond to the temperature at heights above bottom of 4 (lowest line), 24, 44, 64, 84, and 104 m (uppermost line) or 13, 33, 53, 73, 93, and 113 m (Table 1). The thermistor temperature data from 9 July to 26 November 1997 is corrupted (not shown). The only plotted temperature is from the low-resolution ADV sensor at 105 m above bottom (mab).

such that localized cold water masses sink irreversibly to the lake bottom without producing a signal at the mooring. In the following section, we describe such cold intrusion events without, however, identifying the mechanism that caused them.

Cold intrusions—observation and volume estimate of several events

Overview—Observations in the South Basin of the gross sedimentation rate, near-bottom velocity, and near-bottom temperature between December 1995 and November 1997 indicate important seasonal variability (Fig. 4). The deep currents varied from 0 to 10 cm s^{-1}, reaching maximum velocities at the end of the open-water period. They were at a minimum at the end of the ice-covered period. Because the wind is the primary source of mechanical energy, the system is forced only while the lake's surface is open, whereas friction decelerates the system in all seasons (Zhdanov et al. 2001). During the 3½ months of ice cover (113 days in 1996 and 95 days in 1997; marked by asterisks in Fig. 4), the kinetic energy of the deep currents decreased by an order of magnitude (Fig. 4b). The timescale of the decay of the kinetic energy is well defined under the ice cover (Ravens et al. 2000; Lawrence et al. 2002). Plots of water trajectory indicate that the current direction in the deepest 100 m was nearly constant (toward the southeast). We present the observations in detail and provide estimates of the volume of the cold intrusions.

Sedimentation rate—The sedimentation rate is extremely variable, ranging over three orders of magnitude (from ~4 to ~4,000 mg m^{-2} d^{-1}; Fig. 4a). On the basis of this 2-yr record, we conclude that the sedimentation follows a seasonal pattern, with the highest rates during the open-water period (i.e., after the times of spring and fall diatom blooms) and the lowest rates under the ice cover. During the 3½ months of ice cover, the vertical mass flux decreased by 1.5 orders of magnitude. With a linear sedimentation model, the advective timescale of particle settling is about 30 d. Such a timescale corresponds to a settling velocity of about 28 m d^{-1} for the 853-m average depth (Intas Project Team 2002) in the South Basin. The extremely fast settling of the particulate matter is a result of the dominance of diatoms, which are large and dense. For example, filaments of *Aulacoseira baicalensis* are 10–30 μm in diameter and can reach a length of 1.5 mm (Votintsev 1961; Granin et al. 1999).

In addition to the pronounced seasonal pattern, there are two distinctive features in this record. First, the sedimentation rate was greater in the near-bottom trap (1,300 m depth; averaging 549 mg m^{-2} d^{-1}; Fig. 4a, filled bars) than in the 550-m-deep trap (averaging 329 mg m^{-2} d^{-1}; Fig. 4a, open bars). This was especially pronounced in winter 1997, when the lower trap was closer to the sediment. Therefore, we relate this observation to sediment resuspension (Lemmin and Imboden 1987) and subsequent particle redeposition (Grachev et al. 1996). The cold intrusions, which transport particle-containing surface water to great depth (*see next section*), also probably contribute slightly to the increase of sedimentation with depth. Second, the sedimentation rate was much higher in 1997 as a result of enhanced primary production. The diatoms (such as *Aulacoseira baikalensis*) were blooming strongly in 1997 (Mackay et al. 2003). In 1997, the sedimentation rate was extremely high for about 1 month, particularly after the ice break-up (Fig. 4a). Such blooms occur approximately every 3–5 yr under poorly understood conditions, which are also the subject of ongoing research.

Kinematics of individual cold intrusions—The 2-yr observations of near-bottom temperature and velocity provide direct evidence of at least five cold intrusions into the South Basin deep water during the cold period (January to June).

Table 2. List of the individual cold intrusions.

	1–5 Jan 96	15 Jan 96	3 Feb 96	22–26 Jun 96	5–13 Jan 97	1 Feb 97	20–28 Jun 97
Temperature anomaly ΔT (°C) (lower limit)	−0.2	−0.1	0.18	0.08	−0.15	−0.08	−0.1
Duration of intrusion $\Delta\tau$ (days)	3.5	Undefined	1	4	6	Undefined	9
Duration of intrusion for volume calculation $\Delta\tau$ (days)	2	Undefined	1	1	2	Undefined	3
Bottom velocity v (cm s^{-1})	5	2.5	7	3	6.5	4	4
Diameter of intrusion (km)*	9	Undefined	6	3	11	Undefined	10
Intrusion volume V (km^3)†	6	Undefined	3	1	10	Undefined	8

* Estimating the diameter of the intrusion, $v\Delta\tau$, where $\Delta\tau$ is the duration scale of the intrusion and v is the background velocity.

† For the vertical height scale, we used 100 m, because the intrusions were observed over the entire length of the thermistor string. For some volume estimates, this represents an overestimate, for other, an underestimate.

These cold intrusion episodes occurred during 1–5 January 1996, 1 February 1996, 22–26 June 1996, 5–10 January 1997, and 20–28 June 1997 (Fig. 4d; Table 2). In another two instances (15 January 1996 and 1 February 1997), negative temperature anomalies were observed as well, but they immediately followed a larger anomaly, so we suspect we were observing the original cold-water anomaly for the second time. Because of this uncertainty, we claim to have observed six (plus or minus one) cold intrusions during a 2-yr period (3 yr^{-1}).

The different cold intrusion events (Table 2) had unique characteristics in terms of the duration (1 d to 2 weeks), negative temperature anomalies (−0.08 to −0.20°C), height (20 to >100 m vertical extent), velocity (3 to 7 cm s^{-1}), and abruptness of arrival of the intrusions. The analysis of the first intrusion (1–5 January 1996; Fig. 5) indicates that the temperature anomaly of the intruding plume (−0.20°C) and the duration (5 d) were greatest at the bottom of the plume (near the lake sediment). At 104 m above the bottom (mab), the temperature anomaly was still −0.08°C, but the duration was only ~2 d. This suggests that this particular cold intrusion behaved like a density current traveling along the bottom of the basin. The vertical coherence of the thermistor data confirms that the sudden drops in near-bottom temperature are indicative of large-scale transport of water with a character significantly different from that of the ambient water. The velocity was above the annual average during this cold intrusion, consistent with the generally higher velocities at the end of the open-water period (freeze-over was 18 January 1996) and varied between 2 and 9 cm s^{-1} (Fig. 5). That the current direction was southerly before the cold intrusion suggests that it came from the north. At the velocity sensor located 105 mab (midnight, 1/2 January 1996), there was no dramatic change in the velocity (either magnitude or direction) at the time of the arrival of the front. During the strong anomaly of the cold intrusion (first 2 d), the velocity direction shifted counterclockwise (i.e., toward the north). On the basis of the average ambient water velocity (5 cm s^{-1}) and the timescale of the cold intrusion at its midpoint (2 d), the length scale of the intruding plume can be estimated to be ~9 km.

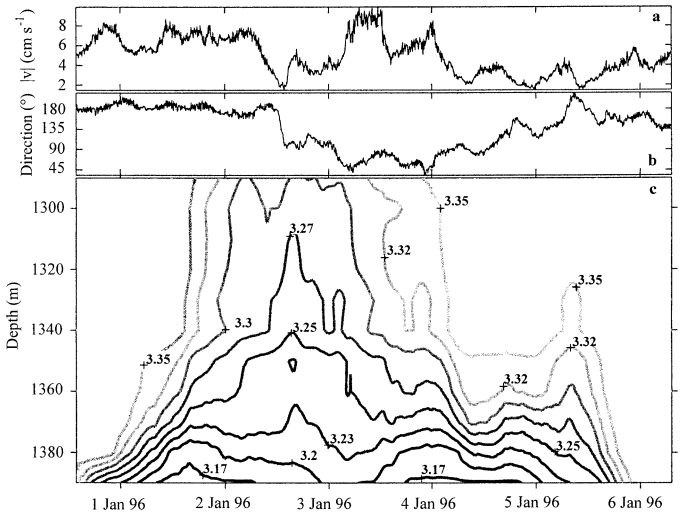

Fig. 5. Details of the cool intrusion from 1 January to 6 January 1996 (Fig. 4d) showing (a) bottom current speed, (b) direction of the bottom currents, and (c) vertical temperature structure (isotherms) from the bottom thermistor chain.

The second event of negative temperature anomaly (15 January 1996) affected only the lowest layer (25 ± 5 m) and lasted an undefined length of time (between 1 and 13 d). This event might have been a remnant of the previous larger event. At the level of the current meter (105 mab), the cold intrusion was observable for only 1 d, but interestingly, the currents made the same counterclockwise turn. Also, the third and forth temperature anomalies (February 1996, June 1996) were very brief (~1 d).

The most effective cold intrusions, in terms of cooling, occurred in 1997. The fifth event (Fig. 6) came in 1-d-long bursts that lasted altogether about 6 d (between 5 and 13 January 1997), again right before the freeze-up of the South Basin. The vertical extent was most probably not much more than 100 m because the uppermost sensor showed a significantly reduced signal. Again, the currents didn't show much correlation with the cold intrusion, although the highest currents occurred during one of the bursts (Fig. 6). The sixth temperature anomaly occurred soon after the fifth event. Unfortunately, we cannot determine whether this constitutes a new intrusion or whether it features the ''wandering'' of previously intruded water masses. Because the signature of the vertical distribution of the temperature anomaly was similar to the previous intrusion, the latter hypothesis is supported. The seventh cold intrusion event, occurring at the end of June 1997, was comparably well defined, with a temperature anomaly of down to −0.08°C and a pronounced current sig-

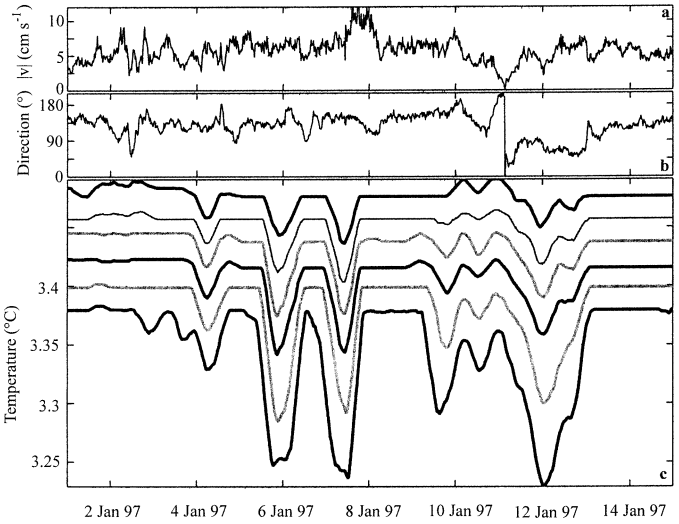

Fig. 6. Details of the cool intrusion from 2 to 14 January 1997 (Fig. 4d) showing (a) bottom current speed, (b) direction of the bottom currents, and (c) temperature from six near-bottom thermistors ranging from 13 to 113 mab.

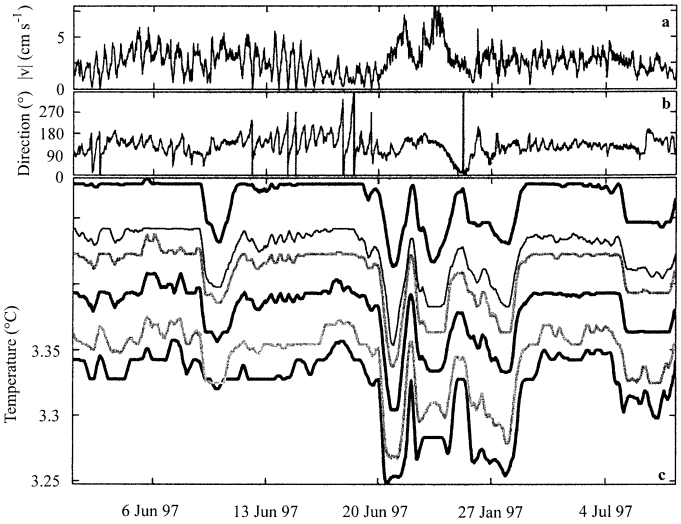

Fig. 7. Details of the cool intrusion from 20 June to 29 June 1997 (Fig. 4d) showing (a) bottom current speed, (b) direction of the bottom currents, and (c) temperature from six near-bottom thermistors ranging from 13 to 113 mab.

nature (Fig. 7). Whereas before and after the cold intrusion, the currents contained a pronounced inertial signature, with a speed of about 2.5 cm s^{-1}, the currents of the cold intrusion were clearly stronger (up to 8 cm s^{-1}), and inertial currents were obviously overrun. The cold intrusion came again in bursts, lasted about 1 week, and was thicker than 100 m and longer than 30 km.

Volume estimates of the cold intrusions—The volume of deep-water input was estimated on the basis of the analysis of individual cold intrusions. It was based on the measured temperature deficit in conjunction with the near-bottom velocity data (Figs. 4–7). The cold intrusions were assumed to be vertically oriented cylindrical plumes of water (consistent with their inertial character; Ravens et al. 2000; Schmid pers. comm.) so that the volume, V, of an intrusion was estimated by $V = \pi R^2 h$, where R is the radius and h is the height of the cold intrusion. The radius estimate was based on the background velocity, v, and the duration ($\Delta\tau$) of the intrusion at its vertical midpoint ($R = 0.5v\Delta\tau$). Note that the duration of the cold intrusion was in some cases estimated to be less than the total duration of the presence of the cold anomaly (Table 2) because it appeared that the same cold water was being recirculated (e.g., Fig. 6). This estimate of the radius would approximate the actual radius if the center of the plume passed over the sensor but would be an underestimate of the plume size otherwise. From this point of view, our estimates could be argued to be a lower limit of the cold intrusion volumes. However, it is probable that the plumes have an oval form (in the direction of the flow; Xu and Moncrieff 1994) instead of a circular one. Therefore, the underestimate might be compensated. The plume height (~100 m) was estimated from the drop-off of the temperature anomaly measured by the thermistor chain (Figs. 5–7).

This approach indicated that individual cold intrusions had volumes ranging from 1 to 10 km^3 (Table 2), with a total annual volume flow of $Q \approx 10$ and 18 km^3 in 1996 and 1997, respectively, in the deepest reaches of the South Basin.

Cold intrusion volume estimates based on seasonal cooling—An alternative estimate of the annual volume of cold intrusions was based on the seasonal change in the deep-water heat content (i.e., the amount of cooling) during the 4-month period from late December to mid- or early April in the winters of 1995/1996 and 1996/1997 (Table 3). For example, the period from 20 December 1995 to 1 April 1996 saw a significant drop-off in the average temperature (about −0.03°C at the near-bottom thermistor chain). In the following year, the near-bottom temperature dropped about −0.05°C in about the same time period. The change in heat content for each period was calculated as $\int \delta T\, dV$ (km^3 °C, the specific heat has been ignored), where δT is the temperature change during the cooling period (based on CTD data), and $\int dV$ indicates integration over the deep-water volume (Table 3; first row). For a defined temperature deficit of ΔT of the cold intrusions, we can estimate the associated volume V of the cold intrusions that led to such a heat deficit: $V = (\int \delta T\, dV)/\Delta T$.

Those V represent underestimates, however, because the effective heat deficit is larger than the observed deficit ($\delta T\, dV$ (km^3 °C). The in situ observed δT in the near-bottom waters (seen in the thermistor and CTD data) is in fact a superposition of cooling effected by the cold intrusions and warming from turbulent diffusion of the warmer water above, as outlined in the introduction. Hence, the actual cooling effected by the cold intrusions is somewhat greater than the observed (net) cooling. The diffusion-induced warming during the period Δt is given by $K_z(\partial T/\partial z)A\Delta t$ (Table 3, second row), where K_z is the vertical diffusivity (Ravens et al. 2000) and A is the basin area at about 100 m above maximum depth (*see footnote in Table 3 for details*). Finally, the intrusion volume is given by $V = [\int \delta T\, dV -$

Table 3. Volume of cold intrusions estimated from seasonal cooling of near-bottom water.

	20 Dec 95 to 1 Apr 96	20 Dec 96 to 15 Apr 97
Net amount of cooling $\int \delta T\, dV$ (km³ °C)*	−1.3	−4.5
Diffusion-related heating of bottom waters (km³ °C)†	0.02	0.2
Intrusion volume V (km³) for $\Delta T = -0.20$ °C‡	6.5	23
Intrusion volume V (km³) for $\Delta T = -0.10$ °C‡	13	45
Intrusion volume V (km³) from Table 2	>9	>10

* The net cooling is based on the average temperature difference, δT, between the beginning and end of the seasonal cold intrusions in the near-bottom water below 1,340 and 1,300 m for the first and second period of cold intrusions, respectively. Temperature data is from thermistor chain and CTD profiles. The observed net cooling reflects the combination of cold intrusions and turbulent diffusion-related warming.

† The heat transport estimate ($K_z\, [\partial T/\partial z]\, A\Delta t$) was made at the upper edge of the zone of apparent heat transport at z = 1,340 and 1,300 m for the first and second cold intrusion period Δt, respectively. The K_z estimate was based on the Osborn (1980) model: $K_z = \gamma_{mix}\, \varepsilon N^{-2}$, where $\gamma_{mix} = 0.2$ and ε = dissipation as estimated from the measured velocity at h = 4 m above bottom and the law-of-the-wall: $\varepsilon(h) = (\tau_0/\rho)(\partial U/\partial h) = u_*^3/\kappa h = C_{4m}^{1.5} U_{4m}^3 \kappa h$ with $C_{4m} = 1.7 \times 10^{-3}$ (Ravens et al. 2000; Goudsmit et al. 1997).

The volume is estimated by dividing the estimated amount of cooling by $\Delta T = -0.20$°C and -0.10°C, respectively.

$K_z(\partial T/\partial z)A\Delta t]/\Delta T$. As seen in Table 3, the cooling from the cold intrusions dominates the warming by diffusion from above, which suggests that the heating and cooling were not in balance during the two cooling periods considered and that the observed cooling is close to the effective cooling caused by the cold intrusions.

For the estimation of V, we have to choose ΔT, which we based on the observed maximum temperature deficit typically of $\Delta T = -0.1$ to -0.2°C (Tables 2, 3). We assume that in a given cooling season, all the intrusions originally had these maximal temperature anomalies. This approach leads to V estimates on the order of 7–45 km³ for the two winter periods, as summarized in Table 3. Because in 1997 further cooling (probably as horizontal mixing homogenized the deep water) was evident after the period of time studied (only one thermistor in Fig. 4d), the cold intrusion volume in 1997 was probably even greater.

It is possible, that V is underestimated by this method if the diffusivities were chosen too small, as Table 3 might suggest. If in 1996 and 1997 the heat in the deep water were in steady state, it would imply that the diffusivity would compensate the observed cooling by about one quarter (1996) and one third (1997) over the considered time periods in Table 3. However, during ice cover, the turbulent mixing is below average and the corrections are subsequently less. Therefore, even for steady-state conditions, the V estimates would be <30% larger. Independent of this uncertainty, we can conclude that the annual volume estimates of cold intrusions, based on seasonal changes in temperature, are comparable to the estimates based on the analysis of individual cold intrusions (Table 3). Both methods indicated a larger cold intrusion volume in 1997 compared with 1996. The total intrusion volume flow in 1996 and 1997 was $Q \approx 10$ and 30 km³ yr⁻¹ (±50%), respectively.

Deep water renewal—summary—It is safe to assume that, in addition to the observed 10–30 km³ intruding annually into the deepest reaches of the South Basin, some additional renewal occurred in shallower zones of the PSDW (below 300 m). The temperature balance at 400 m depth provides a basis for estimating the long-term total annual exchange through the horizontal area in that depth. (The choice of 400 m ensures that no water is horizontally exchanged with the Central Basin; the geothermal heating is negligible.) For steady state, the downward diffusion of heat [$A_{400m}K_{z,400m}(\partial T_{400m}/\partial z)$] is equal to the upward advective transport of heat ($Q_{400m}\Delta T_{400m}$), where $K_{z,400m}$, $\partial T_{400m}/\partial z$, and ΔT_{400m} are the small-scale turbulent diffusivity, vertical temperature gradient, and temperature difference between the deep and the cold intrusion waters, respectively, at 400 m depth (heat capacity is again neglected). The total exchange rate through the area (A_{400m} = 5,460 km²) is given by $Q_{400m} = [A_{400m}K_{z,400m}(\partial T_{400m}/\partial z)]\Delta T_{400m}^{-1}$. On the basis of turbulence measurements and of balancing O_2 and ^{3}He, we chose $K_{z,400m}$ = 12.5 cm² s⁻¹ (Wüest et al. 2000). The vertical gradient $\partial T_{400m}/\partial z$, determined from the 26 CTD profiles of 1996/1997 (listed in the footnote of Table 1), averaged to 0.52×10^{-3} °C m⁻¹. This equation allows us to determine the lower limit of the water exchange, Q_{400m}. If the cold intrusions would have the lowest possible temperature of 0°C (i.e., $\Delta T_{400m} = -3.35$°C), then Q_{400m} = 34 km³ yr⁻¹. For a more realistic temperature difference of $\Delta T_{400m} = -2$°C (typical value at the surface for times of lowest stratification), we get Q_{400m} = 56 km³ yr⁻¹.

As an alternative, the same heat balance of downward diffusion and upwelling can be performed by the differential approach with $(Q_{400m}/A_{400m})\partial T_{400m}/\partial z = K_{z,400m}(\partial^2 T_{400m}/\partial z^2$, where Q_{400m}/A_{400m} is the upwelling velocity at 400 m depth, compensating the intrusion flow Q_{400m} below that depth (Munk 1966). By determining the two derivatives, again based on the 26 CTD profiles (Table 1), and with the use of the same $K_{z,400m}$, the exchange volume flow is given by $Q_{400m} = A_{400m}[K_{z,400m}(\partial^2 T_{400m}/\partial z^2)](\partial T_{400m}/\partial z)^{-1} \approx 50 \pm 20$ km³ yr⁻¹ (Wüest et al. 2000). It is interesting to note that the involved heat flux of ~2.7 W m⁻² is similar to the downward diffusion in the ocean thermocline (Munk and Wunsch 1998).

We conclude that the directly observed cold intrusions carry ~10–30 km³ yr⁻¹ of water from the surface layer (top ~300 m) to the deepest reaches of the South Basin. This flow is lower than the long-term steady exchange of the entire PSDW in the South Basin of approximately 50 ± 20 km³ yr⁻¹ and indicates that only about half of the cold intrusions reach the deepest zones, whereas the other half of the cold intrusions stop higher in the 1,000-m-thick PSDW column of the South Basin. However, the deepest reaches get by far the highest replacement per in situ volume; therefore, the cold intrusions leave the strongest signal there.

Discussion

So far, we have shown that the cold intrusions must come from the surface layer (top 300 m) because only the surface

has sufficiently cold water at the time of the intrusions (Fig. 2). In this section, we argue that the cold intrusions did not have sufficiently high salinity or particle content relative to the ambient water column and, therefore, would be density-deficient relative to the water near the mesothermal maximum. Energetically, the cold intrusions would not be able to pass through the mesothermal maximum and, therefore, would not reach the bottom unless there was some forcing mechanism. Later, we address the question of which processes might be responsible for triggering such cold intrusions.

Density contribution from salinity and particles—Monthly temperature profiles (CTDs measured after ice melt) confirmed the drop in near-bottom water temperature evident in the thermistor chain data. For example, the near-bottom thermistor temperature decline between May 1997 and July 1997 (Fig. 4d) is also seen in the CTD temperature profile data (Fig. 8a). Indeed, one of the temperature profiles (20 June 1997, Fig. 8a) was measured by chance during a significant cold intrusion (Figs. 4d, 7). In order that the cold intrusion (ΔT negative) has sufficient density to sink without a forcing mechanism, the density-deficit associated with such a temperature difference would have to be compensated by a slightly higher salinity ΔS (i.e., $\beta_s \Delta S > \alpha \Delta T$, where β_s is the haline contraction coefficient). This condition would have to be fulfilled at any depth (note that below T_{md}, this relation is always fulfilled because α is positive). For the observed δT in the lowest 161 m (V_{1300m} = 133 km³) of −0.035°C (after the June 1997 cold intrusion), we can calculate (for any given intrusion volume V) the corresponding ΔT (= $\delta T[V_{1300m}/V]$), the required ΔS, and the δS to be observed in situ for the dilution of V/V_{1300m}.

As an example, for V = 8 km³, a temperature deficiency of $\Delta T \approx -0.62$°C would be required, calling for a $\Delta S \approx 6.0 \times 10^{-3}$ psu, which would lead to an increase of salinity in the lowest 161 m of $\delta S \approx 0.34 \times 10^{-3}$ psu. However, the corresponding CTD profiles (Fig. 8b) do not exhibit such changes in salinity—the observed increase is $<0.15 \times 10^{-3}$ psu. In fact, a much larger increase of S would be expected, even without cold intrusions from the dissolution of the settling organic matter alone (Fig. 4a), which was determined by Müller et al. (in press) to ~100 g m^{-2} per season. Also, if we chose much higher volume input, the δS to be expected in situ would always be at least 0.22×10^{-3} psu. Even balancing the entire PSDW body (below 300 m depth) would not change the outcome: The observed δS is even slightly negative, and therefore not compatible with cold intrusions of higher salinity water. Therefore, we conclude that the salinity required to overcome the density barrier close to T_{md} was not detected in the PSDW, and especially not in the deepest layers of the South Basin.

The identical arguments can be applied to the particle concentration. We can determine the particle concentration change ΔP that would be required to compensate for the temperature-related density deficit associated with ΔT (negative) (i.e., $\Delta P > \alpha \Delta T/\beta_P$, where β_P is the density change coefficient; ~0.63 for inorganic particles). Again as an example, for V = 8 km³, a temperature deficit of $\Delta T \approx -0.62$°C would be required, calling for a ΔP of ~5.6 mg L^{-1}, which would lead to an increase of particle content in the lowest 161 m of δP of ~0.34 mg L^{-1}. Given that the particle concentration in the deep water is usually even less (Granina et al. 1995; Potyomkina et al. 1998), such a change of more than ~100% would be easily detectable. Observations of the CTD-based optical backscattering imply that changes in the deep-water particle concentration are not

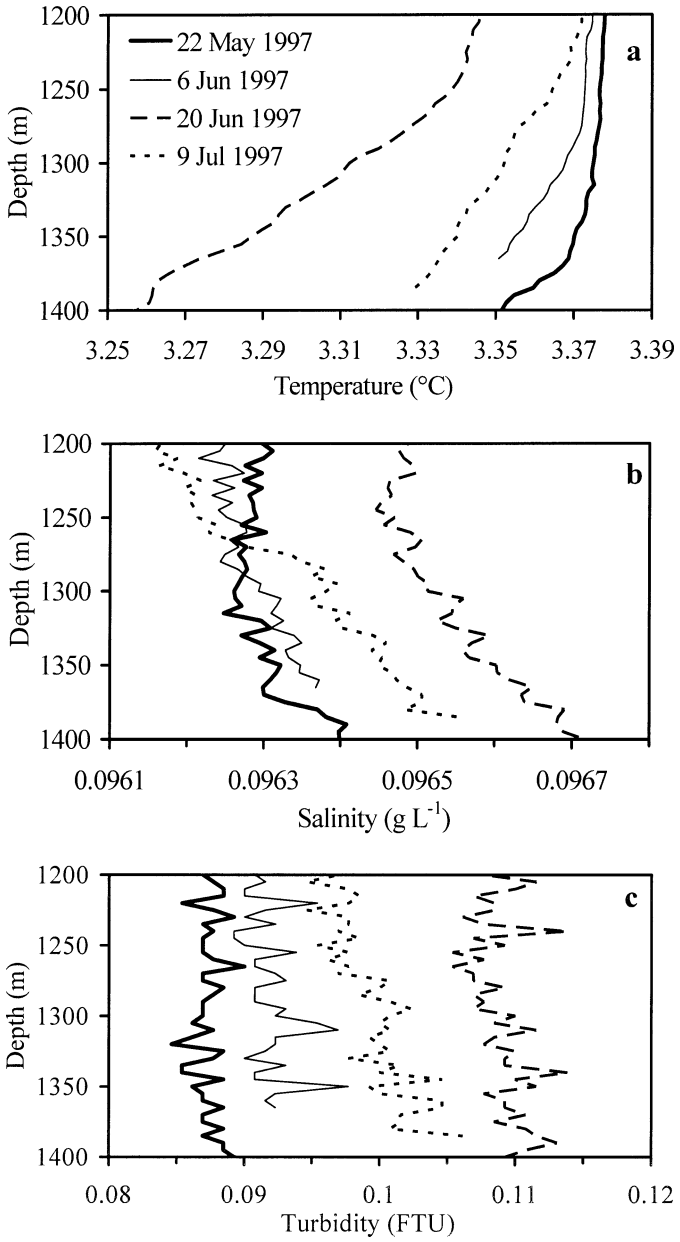

Fig. 8. (a) CTD-based temperature profiles in the lowest 200 m during spring and summer 1997. The 20 June temperature is significantly below the others; explanation is in text. (b) CTD-based salinity profiles in the lowest 200 m as in panel a. (c) CTD-based profiles of optical backscattering in the lowest 200 m measured with an OBS-1. The OBS-1 has been calibrated with a Formazin solution, and the turbidity is given in Formazin turbidity units FTU (~mg L^{-1}).

Table 4. Potential energy barrier for vertical (downward) transport of cold surface water.

Date	Energy barrier for water of $T = 3.25$°C (J m^{-3})	Depth of 3.25°C water (m)	Displacement required (m)
10 Dec 95	3.6	15	240
10 Jan 96	0.98	115	145
5 Mar 96	2.0	80	170
28 Mar 96	1.5	100	160
18 May 96	1.4	100	165
28 May 96	1.3	105	170
3 Jun 96	2.4	0	215
26 Jun 96	1.5	95	170
12 Dec 96	1.7	80	175
13 Mar 97	1.2	115	170
22 Mar 97	0.96	135	155
1 Apr 97	0.87	115	170
22 May 97	1.1	120	170
6 Jun 97	1.1	110	180
26 Nov 97	3.5	5	245

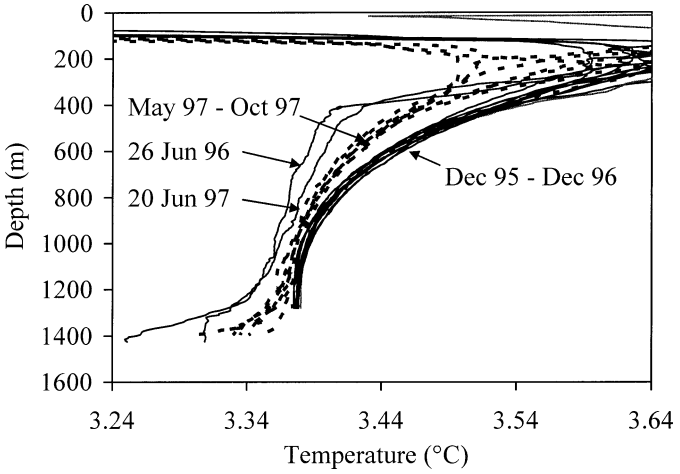

Fig. 9. Temperature profiles from December 1995 to October 1997 demonstrating the existence of ''chimneys.'' The temperature profiles fit into three groups: (1) those profiles taken between December 1995 and December 1996 (excepting 26 June 1996), (2) those taken between May 1997 and October 1997, and (3) those on 26 June 1996 and 20 June 1997, which are significantly colder than normal and suggest chimneys. Temperatures in 1997 (between 400 and 700 m depth) are significantly colder than those in 1996 (consistent with greater incidence of cold-water intrusions).

>1% (Fig. 8c). Although the backscattering in the cold intrusion of 20 June 1997 was slightly higher than seen at other times, the particle concentrations are much too small to overcome the density barrier.

The same calculation for the January 1997 event leaves us with the same conclusion; namely, after the strong cold intrusions, the deep water shows neither associated salinity nor particle increase, which would be required to overcome the density barrier near the mesothermal maximum. Subsequently, we have to conclude that river plunging cannot explain the cold intrusions, although the Selenga River (and other smaller tributaries) typically shows higher salinity during the cold season, when a larger fraction of the flow stems from groundwater (Averin et al. 1992).

Thermobaric instability in the pelagic interior—In summer and fall, the surface water of Lake Baikal follows the classical thermal stratification: The surface is warmer than the PSDW with no possibility of surface-supplied renewal of cold deep water. This is consistent with the absence of cold intrusions during this time of the season (Fig. 4; Table 2). In winter and spring, however, the water column is inversely stratified, with cold water at the top (ice-covered from mid-January to the beginning of May). From mid-December to early June, the surface water is sufficiently cold to be the source of the cold intrusions. However, a potential energy barrier has to be overcome in order to transport colder surface water against the stratification in the top ~270 m. Once the water parcel has reached the critical depth, it can sink freely to the bottom.

In Table 4, we calculated the minimum energy required for 3.25°C water to overcome the stratification. The estimates are based on CTD profiles collected during the cold season. The potential energy is calculated from the upward force $g\Delta\rho'(z)$, which a colder water parcel of a given temperature experiences as it is hypothetically moved downward; $g = 9.81$ m s^{-2} and $\Delta\rho'(z)$ is the density difference between the water parcel to be displaced and the water layers (at depth z) through which the water parcel would be moved. The potential energy barrier is then given by $g \int \Delta\rho'(z)\, dz$, where the integration extends from the depth of $T = 3.25$°C, as observed in the CTD profile (upper limit; second column in Table 4) to the depth at which $\Delta\rho'$ becomes negative (lower limit; Table 4, sum of second and third columns). The lower limit is typically near the location of the mesothermal maximum temperature (~270 m depth). Below that depth, the cooler parcel is heavier than the ambient water and sinks freely to the lake bottom. The estimates in Table 4 represent lower limits because the $T = 3.25$°C water parcels used in the calculations are the warmest that can still effectively cool the bottom waters. The calculations in Table 4 demonstrate that (1) the dates at which the potential energy estimates are minimal occur from early January to mid-June, (2) the minimum energy needed to overcome the stratification is about 1 J m^{-3}, and (3) the vertical displacement is about 160 m (from 115 to 275 m; Table 4).

Indeed, the energy in the internal wave field of lakes is in general ~1 J m^{-3} (Wüest and Lorke 2003), although a slightly smaller energy content has been found for Lake Baikal (Ravens et al. 2000; Schmid pers. comm.). Unfortunately, measurement of the full extent of vertical displacements of the internal waves was restricted because our thermistor chain was deployed between 44 and 144 m depth (Table 1) and the observed internal waves often extended deeper. Nevertheless, measurement of vertical displacements δz that were available were generally, and also specifically during the periods of interest, much shorter (Fig. 9) than required, as indicated by the calculations in Table 4. Also, the energy content of the vertical displacements, $(\rho/2)N^2\, \delta z^2$, is very far

from reaching the critical level. Detailed measurements in later moorings at greater depth demonstrated that at ~280 m depth, the energy content is on average only ~0.01–0.02 J m^{-3} (consistent with maximum displacements of about ±60 m; *see* Fig. 2) and can reach, at most, up to 0.25 J m^{-3} (Schmid pers. comm.).

Baroclinic displacements near the mesothermal maximum did not exceed ~60 m and never reached the required 160 m or more. In addition, our measurements and later measurements never showed enough vertical excitation to overcome the potential energy barrier, which drops to a minimum of about 1 J m^{-3} in January and June. Therefore, thermobaric instability in the pelagic interior is not a relevant process for cold intrusions in the South Basin.

Thermobaric instability at the side boundaries—We consider the side boundary as the most probable location for the formation of cold intrusions penetrating into the deep layers of the PSDW. Ekman pumping provides a mechanism that is realistically able to displace several tens of cubic kilometers of water within days. In contrast to the ocean and other lakes, the stratification in Lake Baikal is very weak; subsequently, not much force is required to displace cold water in such a marginally stratified system.

For simplicity, we consider the stratification of the South Basin as a two-layer structure (which is justified for the relevant cold season) and assume a wind blowing parallel to the shore, creating the regularly observed counterclockwise circulation (Shimaraev et al. 1994). The downwelling is concentrated along the shore to within a distance, given by the baroclinic Rossby radius $c/f \approx 1$ km (Gill 1982), where c is the speed of the first-mode internal gravity wave (~0.3 m s^{-1}) and f indicates the inertial frequency (1.15×10^{-4} s^{-1}). For a surface wind stress τ parallel to the coast, surface water accumulates to the right within this thin boundary; subsequently, downwelling can take place, compensating the inflow (Botte and Kay 2002). The scale of the downward velocity is given by $c\tau/(g\Delta\rho H)$, where $\Delta\rho$ ($\sim 3 \times 10^{-5}\rho$) is the density difference between the surface and the deep water, and H (~270 m) is the thickness of the surface layer. For a typically occurring strong wind in January of 7 m s^{-1} (with corresponding $\tau \approx 0.08$ N m^{-2}), the downwelling velocity reaches >1 m h^{-1}. Because of the extremely weak stratification in Lake Baikal, the downwelling is much faster than for usual oceanic conditions. On the basis of these numbers, we can conclude, that for a strong wind with duration of several days, the Ekman pumping can downwell a volume of several tens of cubic kilometers of cold water. Such winds occur regularly before and after the period of ice cover.

Such a downwelling event probably occurred in June 1997, as indicated by the CTD profiles on 20 June. The important feature of this event is the temperature deficit (~0.02°C) extending all the way to the surface. It resembles the flow chimney described by Walker and Watts (1995), in which cold surface water is transported to the deepest reaches. When the full profile of this chimney, along with that of another (on 26 June 1996), are plotted alongside ''normal'' temperature profiles (December 1995–December 1997), the dramatic nature of these temperature/flow phenomena are apparent (Fig. 9). The comparison of these temperature profiles also indicates that the profiles between 400 and 700 m depth form two groups: those collected between December 1995 and December 1996, which were relatively warm, and those in 1997, which were relatively cold. The cooler profiles in 1997 might be related to the greater incidence of cold intrusions.

Relevance to deep lakes—Near-bottom thermistor data (December 1995–November 1997) indicated the occurrence of cold intrusions into the deepest layers of the South Basin of Lake Baikal in winter and spring when the surface was cooler than the deep water (~3.35°C). The volume of individual cold intrusions ranged from 1 to 10 km^3 per event, and the annual volume flow was estimated to be between 10 and 30 km^3 yr^{-1}, somewhat less than the steady-state estimate for the entire permanently stratified deep water.

Cold intrusions were not accompanied by significant changes in ion or particle content, leaving the Selenga River as a potential source of these components completely unlikely. Two temperature profiles taken during such a cold intrusion indicated lower temperatures throughout the water column. These profiles suggested surface-fed, cold intrusions via thermobaric instability (Walker and Watts 1995). The required downwelling for those plumes definitely did not occur in the pelagic interior of the South Basin but was most probably provided by Ekman pumping, which is expected to be efficient with coast-parallel cyclonic currents (the coast on the right). From the stratification and topographic structure, we can expect that the deep water of the Central Basin (max. depth is 1,642 m) is renewed by identical processes, whereas in the North Basin, horizontal gradients of salinity and temperature can cause thermobaric downwelling (Peeters et al. 1996).

Permanent stratification is a common feature of many deep lakes. For those stratified by long-term temperature gradients, cold intrusions are required to occur on a (more-or-less) regular basis. This is specifically the case for the deep tropical lakes, such as Tanganyika (Verburg et al. 2003) or Malawi (Eccles 1974), in which small temperature differences maintain the permanent stratification during the dry season (Wüest et al. 1996; Vollmer 2002). Although not yet proven, the cold intrusions most probably are a result of plunging of cool and particle-loaded rivers (Soreghan et al. 1999; Vollmer et al. 2002). In temperate regions, however, plunging rivers usually warm the deep hypolimnion, as exemplified in Lake Geneva (Lambert and Giovanoli 1988), and instead contribute to long-term destratification (Loizeau and Dominik 2000). As long as the temperature is above the temperature of maximum density, differential cooling in side basins provide an ideal source of cold intrusions, as documented by Fer et al. (2002).

References

AVERIN, A. I., L. A. GORBUNOVA, AND N. G. GRANIN. 1992. Specific electric conductivity of Selenga River water. Vodniye Resursy **6:** 94–100.

BEETON, A. M. 2002. Large freshwater lakes: Present state, trends, and future. Environ. Conserv. **29:** 21–38.

BOTTE, V., AND A. KAY. 2002. A model of the wind-driven circulation in Lake Baikal. Dynam. Atmos. Oceans **35:** 131–152.

CARMACK E. C., AND R. F. WEISS. 1991. Convection in Lake Baikal: An example of the thermobaric instability, p. 215–228. *In* P. C. Chu and J. C. Gascard [eds.], Deep convection and deep water formation in the oceans. Elsevier.

CHEN, C. T. A., AND F. J. MILLERO. 1986. Precise thermodynamic properties for natural waters covering only the limnological range. Limnol. Oceanogr. **31:** 657–662.

CRAWFORD, G. B., AND R. W. COLLIER. 1997. Observations of a deep-mixing event in Crater Lake, Oregon. Limnol. Oceanogr. **42:** 299–306.

ECCLES, D. H. 1974. An outline of the physical limnology of Lake Malawi (Lake Nyasa). Limnol. Oceanogr. **19:** 730–742.

FER I, U. LEMMIN AND S.A. THORPE. 2002. Observations of mixing near the sides of a deep lake in winter. Limnol. Oceanogr. **47:** 535–544.

GILL, A. E. 1982. Atmosphere—ocean dynamics. International Geophysics Series 30, Academic Press.

GOUDSMIT, G.-H., F. PEETERS, M. GLOOR, AND A. WÜEST. 1997. Boundary versus internal diapycnal mixing in stratified natural waters. J. Geophys. Res. **102:** 27,903–27,914.

GRACHEV, M. A., E. V. LIKHOSHVAY, S. M. KOLMAN, AND A. E. KUZMINA. 1996. Sedimentation flux of diatoms measurements in Lake Baikal with using sequencing trap. Doklady RAN **350:** 87–91

GRANIN, N. G., AND OTHERS. 1999. Turbulent mixing in the water layer just below the ice and its role in development of diatomic algae in Lake Baikal. Dokl. Akad. Nauk SSSR **366:** 835–839.

GRANINA, L. Z., V. B. BARYSHEV, AND A. M. GRACHEV. 1995. Study of elemental composition of suspended sediments in Lake Baikal and its tributaries by X-ray fluorescent analysis based on synchrotron radiation. Nucl. Instrum. Methods Phys. Res. A **359:** 302–304.

HOHMANN, R., R. KIPFER, F. PEETERS, G. PIEPKE, D. M. IMBODEN, AND M. N. SHIMARAEV. 1997. Processes of deep-water renewal in Lake Baikal. Limnol. Oceanogr. **42:** 841–855.

———, M. HOFER, R. KIPFER, F. PEETERS, D. M. IMBODEN, AND M. N. SHIMARAEV. 1998. Distribution of helium and tritium in Lake Baikal. J. Geophys. Res. **103:** 12,823–12,838.

INTAS PROJECT TEAM. 2002. A new bathymetric map of Lake Baikal. Available from: http://allserv.ugent.be/~mdbatist/intas/intas.html

KILLWORTH, P. D., E. C. CARMACK, R. F. WEISS, AND R. MATEAR. 1996. Modelling deep-water renewal in Lake Baikal. Limnol. Oceanogr. **41:** 1521–1538.

KODENEV, G. G. 2001. Deep-water renewal in Lake Baikal. Geol. Geofiz. **42:** 1127–1136.

———, M. N. SHIMARAEV, AND A. T. SHISHMAREV. 1998. Determination of deep-water renewal rate of Lake Baikal using chemical tracers. Geol. Geofiz. **39:** 842–850.

LAMBERT, A., AND F. GIOVANOLI. 1988. Records of riverborne turbidity currents and indications of slope failures in the Rhone delta of Lake Geneva. Limnol. Oceanogr. **33:** 458–468.

LAWRENCE, S. P., K. HOGEBOOM, AND H. L. LE CORE. 2002. A three-dimensional general circulation model of the surface layers of Lake Baikal. Hydrobiologia **487:** 95–110.

LEDWELL, J. R., A. J. WATSON, AND C. S. LAW. 1998. Mixing of a tracer in the pycnocline, J. Geophys. Res. **103:** 21,499–21,529.

LEMMIN, U., AND D. M. IMBODEN. 1987. Dynamics of bottom currents in a small lake. Limnol. Oceanogr. **32:** 62–75.

LOIZEAU, J. L. AND J. DOMINIK. 2000. Evolution of the Upper Rhone River discharge and suspended sediment load during the last 80 years and some implications for Lake Geneva. Aquat. Sci. **62:** 54–67

LORKE A., AND A. WÜEST. 2002. Probability density of displacement and overturning length scales under diverse stratification. J. Geophys. Res. **107:** 3214 [doi:10.1029/2001JC001154]

MACKAY, A. W., R. W. BATTARBEE, R. J. FLOWER, N. G. GRANIN, D. H. JEWSON, D. B. RYVES, AND M. STURM. 2003. Assessing the potential for developing internal diatom-based transfer functions for Lake Baikal Limnol. Oceanogr. **48:** 1183–1192.

MUNK, W. H. 1966. Abyssal recipes. Deep-Sea Res. **13:** 707–730.

———, AND C. WUNSCH. 1998. Abyssal recipes II: Energetics of tidal and wind mixing. Deep-Sea Res. **45:** 1977–2010.

MÜLLER, B., M. MAERKI, M. SCHMID, E. G. VOLOGINA, B. WEHRLI, A. WÜEST, AND M. STURM. In press. Internal carbon and nutrient cycling in Lake Baikal: Sedimentation, upwelling and early diagenesis. Global and Planetary Change.

OSBORN, T. R. 1980. Estimates of the local rate of vertical diffusion from dissipation measurements, J. Phys. Oceanogr. **10:** 83–89.

PEETERS F., G. Piepke, R. Kipfer, R. Hohmann, and D. M. Imboden. 1996. Description of stability and neutrally buoyant transport in freshwater lakes. Limnol. Oceanogr. **41:** 1711–1724.

———, R. KIPFER, M. HOFER, D. M. IMBODEN, AND V. M. DOMYSHEVA. 2000. Vertical turbulent diffusion and upwelling in Lake Baikal estimated by inverse modeling of transient tracers. J. Geophys. Res. **105:** 3451–3464.

POTYOMKINA, T. G., V. B. BARYSHEV, A. M. GRACHEV AND V. L. POTYOMKIN. 1998. Chemical composition of suspension in water body of Lake Baikal. Nucl. Instrum. Methods Phys. Res. A **405:** 543–545.

RAVENS, T. M., O. KOCSIS, A. WÜEST, AND N. GRANIN. 2000. Small-scale turbulence and vertical mixing in Lake Baikal. Limnol. Oceanogr. **45:** 159–173.

SHIMARAEV, M. N., AND V. M. DOMISHEVA. 2002. Dynamics of dissolved silica in Lake Baikal. Dokl.-Earth Sci. A **387:** 541–544.

———, AND N. GRANIN. 1991. Temperature stratification and the mechanism of convection in Lake Baikal. Dokl. Akad. Nauk SSSR **321:** 831–835.

———, ———, AND A. A. ZHADANOV. 1993. Deep ventilation of Lake Baikal due to spring thermal bars. Limnol. Oceanogr. **38:** 1068–1072.

———, V. I. VERBOLOV, N. GRANIN, AND P. P. SHERSTYANKIN. 1994. Physical limnology of Lake Baikal: A review. Okayama Irkutsk.

SOREGHAN, M. J., C. A. SCHOLZ, AND J. T. WELLS. 1999. Coarse-grained, deep-water sedimentation along a border fault margin of Lake Malawi, Africa: Seismic stratigraphic analysis. J. Sediment. Res. **69:** 832–846.

VOTINTSEV, K. K. 1961. Hydrochemistry of Lake Baikal. Izdanija AN SSSR, Moscow. (In Russian)

VERBURG, P., R. E. HECKY, AND H. KLING. 2003. Ecological consequences of a century of warming in Lake Tanganyika. Sciences **301:** 505–507.

VOLLMER, M. K. 2002. Studies of deep-water renewal in Lakes Malawi/Nyasa and Issyk-kul using sulfur hexafluoride and chlorofluorocarbons as time-dependent tracers. Thesis, Univ. of California, San Diego.

———, R. F. WEISS, AND H. A. BOOTSMA. 2002. Ventilation in Lake Malawi/Nyasa, p. 209–233. *In* E. O. Odada and D. O. Olago [eds.], The East African Great Lakes: Limnology, paleolimnology and biodiversity. Kluwer.

WALKER, S. J., AND R. G. WATTS. 1995. A three-dimensional numerical model of deep ventilation in temperate lakes. J. Geophys. Res. **100:** 22,711–22,732.

WEISS, R. F., E. C. CARMACK, AND V. M. KOROPALOV. 1991. Deep-water renewal and biological production in Lake Baikal. Nature **349:** 665–669.

WÜEST, A., G. PIEPKE, AND J. D. HALFMAN. 1996. Combined effects of dissolved solids and temperature on the density stratification of Lake Malawi, p. 183–202. *In* T. C. Johnson and E. O. Odada [eds], The limnology, climatology and paleoclimatology of the East African lakes. Gordon and Breach.

———, N. GRANIN, O. KOCSIS, T. M. RAVENS, M. SCHURTER, AND M. STURM. 2000. Deep water renewal in Lake Baikal—matching turbulent kinetic energy and internal cycling. Terra Nostra **2000:** 60–74.

———, AND A. LORKE. 2003. Small-scale hydrodynamics in lakes. Annu. Rev. Fluid Mech. **35:** 373–412.

XUE, Q., AND M. W. MONCRIEFF. 1994. Density-current circulations in shear flows. J. Atmos. Sci. **51:** 434–446.

ZHDANOV, A. A., N. G. GRANIN, AND M. N. SHIMARAEV. 2001. The generation mechanisms of under-ice currents in Lake Baikal. Dokl. Earth Sci. **377A:** 329–332.

Received: 23 December 2003
Accepted: 14 June 2004
Amended: 26 July 2004